

# **Finite Element Analysis of TDR Cable-Grout-Soil Mass Interaction During Localized Shearing**

By J. Tanner Blackburn<sup>1</sup> and Charles H. Dowding<sup>2</sup>

Keywords:

Time Domain Reflectometry, Three-Dimensional, Finite Element, Modeling, Cylindrical Composite, Tunnel, Localized Shear Failure, Shear Displacement, Shear Deformation Surveillance

## ***Abstract***

Three-dimensional finite element analysis is combined with field and laboratory measurement of Time Domain Reflectometry (TDR) cable-grout response to analyze the interaction between the cable, grout, and surrounding soil mass during localized shearing. Finite element (FE) model parameters for the cable and cable-grout interface elements are back-calculated by matching results from laboratory shearing tests to FE calculated response. These parameters are employed in subsequent FE model geometries to model the behavior of TDR cable-grout composites in soft soils. Optimal grout and cable design is determined by analyzing the relationship between grout strength and stiffness and calculated cable shear stress.

## ***Introduction***

This paper describes the combination of laboratory and field measurements with three dimensional (3D) finite element modeling for the analysis of the interaction of a variety of TDR cable-grout systems in a variety of surrounding soils. Finite element analysis was necessary to overcome the obvious difficulty of developing a laboratory device large enough to shear the TDR cable-grout hole-soil composite containing a 20 mm diameter TDR cable in a 100 mm bore hole. A two ring shear device designed to

---

<sup>1</sup> Grad. Res. Asst., Dept. of Civ. and Env. Engrg, Northwestern Univ., Evanston, IL 60208.

<sup>2</sup> Prof., Dept. of Civ. and Env. Engrg., Northwestern Univ., Evanston, IL 60208.

properly surround the bore hole with soil would require a minimum inner diameter of 400 to 500 mm and a length of 1 to 1.5 meters. Controllably creating multiple large soft clay samples to fill the device would be even more difficult and expensive than building the device. Conducting a number of *in-situ* experiments would be even more difficult than building, filling, and operating a laboratory device.

The analyses described herein were necessary to begin to develop the technology necessary to employ TDR cables to measure deformations in soil with the same degree of success as in rock. More specifically the experiments and analyses were meant to test the hypothesis that there is an optimum grout strength for a given cable stiffness and soil strength. Installations of TDR cable-grout composites in stiffer rock that deforms locally along joints have successfully detected and monitored localized shear displacement (Dowding and Huang, 1994), which has led to widespread use of TDR cable technology in the mining industry. Lack of well instrumented installations in soil, as well as differences in failure mechanisms and relative stiffnesses of rock and soil, have inhibited development of optimal cable-grout composites for use in soil.

Analysis of TDR cable-grout-soil interaction is presented in the following order: 1) discussion of the results of a field case study comparing TDR cable and slope inclinometer response to localized failure in soft clay, 2) comparison of laboratory results of shearing of individual cables and cable-grout composites with three dimensional finite element model results, and 3) analysis of three dimensional finite element modeling of cable-grout-soil composite interaction in soft to medium soils.

### ***Field Measurement of Localized Shear Failure in Soft Clay***

This case history, which shows the comparative response of TDR cables and slope inclinometers in soft soil, involves the failure of a land fill located over 12 to 15 meters (40-50 ft) of soft, glacial lacustrine clay. As shown in Figure 1, localized shear failure was concentrated in the soft clay layer, at a depth of 27 to 31 meters (90-100 ft). This localized shearing was monitored with two slope inclinometers and two TDR cable-grout composites to compare responses. Data were collected for nearly two years.

Response of the two cables differed significantly during the slope deformation that followed installation. Between April, 1998 and February, 2000 the thinner (8 mm), braided outer conductor cable (Cable B) with stronger grout, did not respond to deformation, while the thicker (22 mm), solid outer conductor cable (Cable A) with weaker grout did. Responses of TDR Cable A, in the form of the full wave form, are compared to inclinometer responses in Figure 2.

The largest responses occurred at depths of 28 and 30 meters (92 and 99 ft), which, as shown in Figure 2, exist in the zones of highest incremental and cumulative displacement measured with the inclinometer. The shallower region of large displacement at approximately 8 meters does not have a corresponding TDR response. One possible explanation is that since the TDR cable and inclinometer were separated by approximately thirty meters (as shown in Figure 1) the two instruments were in different blocks sliding on the same shear zone and that the shear plane between the two blocks intersected the slope inclinometer.

Responses shown in Figure 2 demonstrate that TDR cable technology can detect localized shearing of soft soil. However, differences in responses of Cable A and B demonstrate the need to properly design TDR cable-grout composites for use in soft soil. Analysis of cable-grout-soil interaction during shearing, described herein, will help demonstrate why one TDR cable-grout composite (Cable A) was successful in detecting shear displacement, while another configuration (Cable B) was not.

This case history shows that both TDR cables and slope inclinometers measure deformation in soil, and that the measurements differ. As has been discussed elsewhere (Dowding and O'Connor, 2000), slope inclinometers are more sensitive to general shear or tilt and TDR cables are more sensitive to localized shear. As such, each has its unique capabilities. It is therefore important to determine how the positive attributes of each, separately or in combination, can be exploited to better understand deformation of soil and rock masses.

## **Laboratory Shearing of Cable and Cable-Grout Composites for Model Calibration**

This section describes three-dimensional (3D) finite element analysis (FEM) of laboratory shearing of Time Domain Reflectometry (TDR) cables and cable-grout composites to determine appropriate constitutive properties for 3D analysis of interaction between the cable-grout composite and surrounding soil mass. This interactive analysis is necessary to determine the most sensitive combination of cable and grout properties for TDR measurement of localized shearing in soft soil under field conditions.

Three different laboratory tests were conducted to measure the properties of the 1) cable, 2) grout, and 3) cable-grout composite (Cole, 1999 and Dowding et. al., 2001). The cables themselves were double ring sheared to measure their force-displacement response. The weak cement-bentonite grouts employed in the composites were sheared in unconfined compression to determine their constitutive properties. Lastly, the cable-grout composites were sheared in a large, three ring shear device to measure the composite force-displacement response, cable-grout interface properties, and the TDR voltage reflection-displacement response.

Cable and grout constitutive properties, and cable-grout interface properties, were obtained by a combination of laboratory tests and FE model calculations. First, an appropriate 3D FEM model of the apparatus for shearing the cables was created and employed to determine the constitutive properties of several cables. The laboratory cable shearing test mimics a direct shear soil test, which does not provide a constitutive relationship (because of poorly controlled boundary conditions). Therefore, the cable constitutive properties were obtained by matching calculated and measured force-displacement curves. The cable constitutive properties were then employed in the 3D FEM models of laboratory shearing of cable-grout composites in order to back-calculate the interface properties between the grout and cable. Finally, the back calculated grout strength (which is not used in the analysis) is compared with the strength obtained by unconfined compressive strength tests to validate the procedure for back-calculation.

Finally, a critical shear stress in the cable for initial TDR response was determined from the 3D FEM models of the laboratory shearing of the cable-grout composite. It is the calculated cable stress in the cable-grout composite at the minimum deformation for which the laboratory composite produced the first TDR voltage

reflection. It will be employed in the next section for comparison with cable shear stresses calculated with the complete 3D FEM model of localized shearing through the cable-grout-soil composite in the field.

The FEM analysis of laboratory tests is described in the following order: (1) 3D Finite Element Analysis Software description, (2) FEM modeling of the cable shear test, (3) FEM modeling of the cable-grout composite shear test, and (4) back calculation of constitutive properties from the finite element results.

### **Plaxis 3D Tunnel – Finite Element Analysis Program**

A commercial Three-Dimensional Finite Element Package, Plaxis 3-D Tunnel (Plaxis, 2001), is employed to model the behavior of coaxial cables, cable-grout composites and finally the cable-grout-soil interaction. This special purpose three-dimensional finite element software package is designed for axially symmetric geometries such as cables, pipes, and tunnels. The automatic 3D mesh generation feature and graphical display of results simplified the tedium of mesh creation and interpretation involved with complex 3D interactions.

The three-dimensional automatic mesh generation procedure allows for local refinement and generation of the mesh, in three dimensions, with little computational effort. As shown in Figure 3, the input procedure begins by defining the geometry of a two-dimensional cross-section (slice) of the model, which is formed into a two-dimensional mesh consisting of six-noded triangular material elements and ‘zero-thickness’ interface elements. Interface elements have no thickness, but have shear stiffness and strength properties that can be specified independently of the material elements. From this cross-section the three dimensional mesh is produced by extruding the two-dimensional ‘slices’, in the axial direction, with different thicknesses. The thicknesses of the compiled slices are restricted by Plaxis, according to the coarseness of the two-dimensional mesh to avoid computationally unstable thin elements. An apparent thickness limit of ten times the smallest element width is set by Plaxis. Material elements, prescribed displacements, and tractions can be changed for each individual slice, which allows modeling the different soil and cable properties in both the radial and axial directions. For additional information regarding mathematical and technical details

of Plaxis 3D calculation procedures the reader is referred to the users manual (Plaxis, 2001).

Plaxis 3D Tunnel offers a variety of material models. The Mohr-Coulomb material model, which employs a linearly elastic-perfectly plastic idealized material behavior, is used in this analysis. The Mohr-Coulomb material model does not account for the effect of stress history or time effects. However, the Mohr-Coulomb material model does allow plastic deformation once the material element has yielded. The plastic deformation will be evident in the resultant force-displacement curves, shown later.

### **Laboratory Cable Shear Test**

To determine the shear strength and stiffness of coaxial cables used in Time Domain Reflectometry, a double ring shear apparatus was devised that would hold a variety of larger diameter coaxial cables (~ 2 centimeter diameter) (Bilane,1994). An interior aluminum block slides up and down within a larger, restraining aluminum block to transversely shear the cable at one location. A gap of approximately one millimeter exists between the large, stabilizing block and the smaller, moving block. The smaller block is displaced relative to the large stationary box by a piston to produce the force-displacement response.

Although the shearing device was used to measure the shearing response of a variety of TDR coaxial cables (Cole, 1999), only two optimum cables and the corresponding test results are modeled in the following finite element analysis. The two cables, shown in Figure 3, in this analysis differ significantly in their construction and deformability: a stiff cable with a solid outside conductor and a compliant cable with a braided outside conductor. The outer radius of both cables is approximately twenty two millimeters (solid outer conductor,  $r = 22.23$  mm; braided outer conductor,  $r = 21.85$  mm).

A commercially available coaxial cable, Commscope Parameter III 875 Cable commonly used in TDR measurements, provided the base stock for the two alternatives. It is composed of a solid aluminum outer conductor, foam polyethylene dielectric, and a copper-clad, aluminum inner conductor. The solid aluminum outer conductor provides

excellent electrodynamic properties for TDR; however, it increases the cable stiffness; therefore this cable is optimal for stiffer media (Dowding et. al., 2001, Cole, 1999).

The second coaxial cable is a modified Commscope Parameter III 875 Cable. The outer aluminum conductor has been stripped and replaced with a tin/copper braid (Alpha 2176) and heat shrinkable, PVC sheathing. The braided outer conductor results in a more compliant cable and provides adequate electrodynamic properties. Throughout this report the cables will be referred to as “Solid Cable” and “Braided Cable”, which refers to the outer conductor. The braided cable described in this section and discussed in future sections is different from the braided cable employed in the field case; it is larger in diameter with higher density braiding.

This laboratory shear test mimics a direct shear test, which does not allow determination of the constitutive properties of the material. This limitation results from stress discontinuities and poorly defined boundary conditions inherent in the direct shear configuration. Therefore, the cable constitutive properties were obtained by matching measured (laboratory) and calculated (FE) Force-Displacement relations.

### **Finite Element Analysis of Cable Shear Test**

By matching measured force-displacement curves with the results from a three dimensional finite element model, shown in Figure 4, appropriate values of constitutive parameters are determined for these cable types. Model geometry consists of right and left blocks with the material properties of aluminum, separated by one millimeter; the coaxial cable, modeled as one continuous unit, passes through each aluminum block. The right aluminum section is fixed in the vertical direction, whereas the left aluminum section has a prescribed displacement in the vertical direction at the location corresponding to the piston in the laboratory model. Model geometry only consists of half of the laboratory shear test apparatus due to model symmetry. Presentation of results with this half model enables observation of cable behavior inside the aluminum apparatus.

Mohr-Coulomb material parameters that are variable in this analysis are the modulus of elasticity (E) and the cohesion (c) of the coaxial cable. Parameters that remain constant are the Poisson’s ratio ( $\nu=0.2$ ) and friction angle ( $\phi=0^\circ$ ); additional

parametric studies show that  $\nu$  and  $\phi$  have relatively small effects on the resultant curves (Blackburn, 2002). Aluminum blocks are assigned material properties that represent actual aluminum; however, as long as the aluminum blocks have a considerably higher modulus of elasticity and strength, the material properties of the blocks are insignificant. For instance, the modulus of elasticity for aluminum is 70,000 MPa versus 75 MPa for the stiffer, solid aluminum cable.

Material parameters for both the solid and braided cables are acquired by adjusting the cable's constitutive properties until the computed finite element force-displacement response fits the measured response during laboratory shearing. The deformed finite element mesh in Figure 4 shows the relative displacement and shearing of the cable inside the aluminum blocks. Figure 5 compares the best fit calculated responses for the solid and braided cables with those measured. The finite element model responses lack the gradual curvature seen in the laboratory results in part because the behavior is idealized as linear elastic-perfectly plastic by the Mohr-Coulomb material and interface models. The modulus of elasticity and cohesion (strength) properties of the cable are determined by matching the measured initial elastic and ultimate strength responses. These parameters are used in the finite element models of cable-grout composites described in the next section, which incorporate interaction between the coaxial cable and surrounding grout, and are listed in Table 1.

### **Laboratory Cable-Grout Composite Shearing**

Shear response of various coaxial cable-grout composites have been measured by shearing the three-part cylinder in Figure 6 with a modified controlled displacement loading device (Cole, 1999). Composite cylinders are 100 mm in diameter to simulate common bore-hole sizes with the 20 mm diameter coaxial cable grouted into the center. The finite element model of the right shear zone is shown in Figure 7. End sections of the cable-grout composite cylinder are placed in saddles to brace the cylinder while the center section is displaced downward. The downward displacing piston is fitted with a curved steel frame, to distribute the load across the center cylinder section. Dial gauges monitor vertical (shear) displacement of the center section, relative to the ends and a proving ring monitors vertical force required to displace the center section. Gaps



between the end sections and the center are between 5 and 10 mm. The open ends of the composite cylinder allow for TDR signals to be transmitted and recorded.

During shearing the TDR signal reflection amplitude versus relative displacement across the shear zone was recorded by Cole (1999). These reflection-displacement relations were employed to determine the minimum shear deformation in the cable at the shear zone necessary to produce a measurable reflection. This approach was also employed by Cole (1999) to measure the load-deformation response of composites from a wide variety of different cable types and grout strengths.

Composite shear response for both solid and braided cables is shown in Figure 8 in the forms of vertical force and TDR signal reflection amplitude versus relative displacement across the shear zone. These particular responses are for cable-grout composites with the most compliant grout that is just stiff enough to produce a TDR voltage reflection by shearing the cable. Constitutive properties for the grout had also been independently measured through unconfined compression (Cole, 1999).

The minimum cable deformation (or shear stress) required to generate a TDR response is an important parameter for modeling cable-grout-soil mass interaction at the shear zone. This critical parameter can be determined by matching model and laboratory results for TDR reflection versus transverse, relative displacement of the composite as shown in Figure 8. The responses are for solid and braided cables surrounded in grouts with cohesion values ( $c_{\text{grout}}$ ) of 300 kPa grout and 200 kPa grout, respectively. The grout is modeled as a frictionless ( $\phi=0^\circ$ ) material, therefore the cohesion is equal to half the unconfined compression strength. There are two lines shown for each cable type in Figure 8b, corresponding to the right and left shear zones in the laboratory apparatus. The measured minimum relative displacement necessary for TDR reflection for the solid cable can be distinguished from Figure 9a. The TDR reflection is immediately apparent for the right shear zone of braided cable, yet requires four millimeters of relative displacement to become apparent for the left shear zone of braided cable. The discrepancy in displacements and the immediate TDR reflection is probably the result of rotation of the center section. Therefore the minimum relative displacement is determined by drawing a 'best fit' line through the sloping TDR response lines, using the x-axis

intercept as the minimum relative displacement. A similar approach is used for the solid aluminum cable results to determine the minimum relative displacement of the composite.

Cable shear stress, or cable deformation (curvature), calculated with the 3-D model at the minimum “measured” relative displacement to provide a TDR reflection can be employed as a criterion for modeling the interaction of TDR composites and surrounding soil in subsequent analyses. By displacing the cylinder section of the cable-grout composite in the finite element model of the composite in Figure 7 an amount equal to the laboratory test displacement, the associated shear stress levels in the cable are calculated. Further discussion of these critical cable shear stress levels will follow in the next section that describes the finite element analysis.

### **Finite Element Analysis of Grout-Cable Composite Shear Test**

As shown in Figure 7, only one of the two shear zones was modeled with a fixed end section and the displaced middle section. The left cylinder section is given a prescribed displacement at the point of contact between the proving ring and the steel frame. As described before, all materials are considered to be elastic-perfectly plastic using the Mohr-Coulomb yield criteria. Interface elements between the cable and grout allow relative movement between the grout and cable and are modeled by applying reduction factors to the cable properties. The external restraint (braced PVC pipe) is not included in the FE model because the interface properties between the grout and PVC are not necessary for the soil-grout-cable analysis.

The finite element model is executed several times, with the following goals: (1) the model is displaced enough to match the laboratory measured force-displacement curves and (2) the model is displaced the minimum measured relative displacement needed to generate a TDR response in the laboratory tests. The second displacement is undertaken to calculate cable deformation and shear stresses generated in the cable at the time of the first TDR reflection.

Grout strength and stiffness parameters are back-calculated by matching calculated response of solid and braided cables with force-displacement curves measured in the laboratory, as shown in Figure 8a. The back-calculated grout strength and stiffness

parameters are compared with unconfined compression test results to validate the back-calculation process, but are not used in the cable-grout-soil composite analysis. The material model used in this analysis does not describe post-failure softening of the braided cable response. However, the initial stiffness and yield point of the laboratory results are faithfully reproduced. The back-calculated grout strength and stiffness parameters are listed in Table 1.

Interface constitutive parameters between the grout and cable are found by an optimization process that attempts to match the calculated and measured force-displacement curves (as shown in Figure 8a) and grout-cable separation (shown in Figure 9) in so far as possible. Back-calculated parameters are the shear modulus of the interface elements,  $G_{inter}$ , and the cohesion of the interface elements,  $c_{inter}$ . The interface shear modulus affects the ‘slip’ and the ‘separation’ between the grout and cable materials during relative displacement. Cable-grout interface stiffness and strengths are calculated by applying reduction factors to the cable properties. Because the material models used in the finite element model have zero friction angles, the shear strength of the interface elements is equal to their cohesion. The two back-calculated interface parameters for each cable are also listed in Table 1.

Table 2 compares: 1) the grout strength determined by finite element analysis to that measured by unconfined compression and 2) the grout-cable separation observed in the finite element analysis and that observed during laboratory shearing.

In addition to obtaining interface parameters, the finite element model provides information regarding the change in cable geometry and shear stresses produced in the cable during relative displacement between the left and right composite sections. Calculated shear stress acts in the transverse direction on the plane normal to the axial direction ( $\sigma_{zy}$ , with axes shown in Figure 7). The value of shear stress reported in Table 1 is that calculated in the cable at the minimum relative displacement necessary to generate the first TDR response (critical shear stress). Calculated shear stress in the cable is compared with the critical shear stress during the analysis of the soil-grout-cable interactions to estimate the likelihood of generating a TDR response to the shearing.

## ***Finite Element Analysis of Soil-Grout-Cable Interaction***

Measurement of localized shear displacement in soft soil with Time Domain Reflectometry (TDR) cables requires use of an optimum combination of cable and grout properties for a given soil condition. In this section three-dimensional (3D) finite element (FEM) analyses of the interaction of cable-grout composites with the surrounding soil are employed to determine the optimum combination. The critical property that allows the extrapolation of laboratory to field response is minimum shear stress in the cable, or maximum curvature of the cable, associated with the first TDR reflection. Details of these property determinations were described in the previous section.

Optimum cable design is constrained by two dominant failure mechanisms: 1) grout that is too weak (compliant) to shear the cable sufficiently to produce a signal reflection and 2) a cable-grout composite that is too strong (stiff) and causes the soil mass to shear around, rather than through, the composite (and cable). By analyzing a variety of cable, grout, and soil combinations, the appropriate cable can be paired with an optimally stiff grout to produce the critical shearing stress in the cable. This optimum design provides a grout with enough strength (stiffness) to adequately deform the cable, yet is weak (compliant) enough so as to limit failure in the surrounding soil mass.

The FEM analyses of the interaction between the cable-grout composite and surrounding soil is described in the following order: 1) development of model geometry and loading, 2) assignment of material parameters, 3) model operation with incrementally changed grout properties, 4) comparison of results to critical shear stress levels determined in the previous section, and 5) discussion of optimal grout and cable selection based on FEM results and comparisons.

### **Finite Element Model and Properties**

As before, the process for defining an initial geometry begins by creating a two-dimensional slice, which is then extended to three dimensions by adding slices perpendicular to the plane of this view, as shown in Figure 10. Although the interface elements have zero thickness they are expanded to be visible graphically. A 100 millimeter diameter borehole was employed to define the cable-grout composite, with a

cable diameter of 20 millimeters. Both of these geometrical parameters were held constant throughout the analysis. This geometry is that of composites and cables typically employed in the field. The cable diameter is that of widely used, commercially available cable and similar to that employed in laboratory testing. The soil mass is 300 millimeters wide, 600 millimeters high, and 750 millimeters long. Because of axial symmetry only an axial half of the cable-grout-soil composite need be modeled.

To simulate the shearing soil mass, a prescribed displacement is applied to the top of the slices for the left half of the model in Figure 10, with the bottom of these slices left free. The top of the left soil mass was displaced downward fifteen millimeters, equal to three quarters of the cable diameter. The right half of the model is fixed at both the top and bottom. The halves are separated by a 5 mm thick shear zone, which is modeled with a linear elastic material that is several orders of magnitude softer than the surrounding soil.

The strength and stiffness for the interface between the borehole grout cylinder and surrounding soils are specified as a fraction of the grout properties. For example, the interface strength is assigned a value that is 0.66 times the soil strength. This fraction was held constant for all analyses. Further parametric analysis (Blackburn, 2002) shows that the resulting shear stress in the cable is not significantly affected by varying the interface strength and stiffness between the grout and the soil from these values.

The constitutive properties of the 5 mm thick compliant shear zone are as follows: friction angle,  $\phi=0^\circ$ ; Poisson's Ratio,  $\nu=0.2$ ; and modulus of elasticity,  $E=100$  kPa. The modulus of elasticity is two orders of magnitude lower than the softest soil material used, which has a modulus of elasticity of 12,500 kPa, and allows for large shear displacements in the shear zone without yielding. The friction angle ( $\phi$ ) and Poisson's Ratio ( $\nu$ ) were held constant throughout the analysis, as they were for the soil, grout, and cable material elements.

Optimum grout strengths for solid and braided outer conductor cables were determined for soft to medium, medium to stiff and stiff clays. For a given soil strength and modulus of elasticity, incremental values of grout shear strength ( $c$ ) were varied from 25 kPa to 400 kPa in the TDR composite model. The soil strengths represented: (1) a

soft to medium clay [ $c=25$  kPa], (2) a medium to stiff clay [ $c=50$  kPa], and (3) stiff clay [ $c=100$  kPa]. The soil stiffness assigned by assuming a modulus of elasticity to strength ratio of 500 (Ladd, et. al., 1977). Therefore the respective moduli of elasticity were 12,500 kPa, 25,000 kPa, and 50,000 kPa.

### **Model Response**

The deformed three-dimensional mesh after 15 mm of relative displacement is shown in Figure 11, with shaded transverse shear stresses ( $\sigma_{zy}$ ) in the cable. The greatest shear stresses in the cable, which occur in the region of the shear zone, depend on the relative strength (and stiffness) of the cable, grout, and soil, as well as the magnitude of relative displacement.

Optimum grout strength for the two cables in three soils can be found from the comparison of calculated shear stress in the cable as a function of the grout strength in the upper row of graphs in Figure 12. The optimal grout strength for a specific soil strength corresponds to region 2, shown in the upper middle graph of Figure 12. Shear stress levels in the cable that are ‘less-than-optimal’ correspond to regions 1 and 3. Shear stresses are too low for one of two reasons as discussed above: (1) the grout is too compliant to shear the cable (region 1 in Figure 12) or (2) the cable-grout composite is too strong, causing the soil adjacent to the shear band to fail around the composite (region 3 in Figure 12). Critical shear stress levels to produce a minimum TDR voltage response, discussed in the previous section, are shown as dashed lines in Figure 12.

Consider the shear failure of the soil around the cable-grout composite, shown in region 3 of Figure 12. The extent of large soil strains around the stiff composite can be estimated by tracking the width (in the axial direction) of the zone of two percent shear strain ( $\gamma_{xy}$ ) around the composite. The lower row of graphs in Figure 12 compares the growth in width (in the axial direction) of the two percent soil strain around the composite as the grout strength increases from behavior region 1 to 2 to 3 for each soil strength. In a medium to stiff soil with solid cable the high strain zone grows from 5 mm at the optimum (100 kPa grout) to 200 mm for 350 kPa grout.

Next consider the shear failure of weak grout around the cable, typified by region 1 in the upper row of Figure 12. In this case the grout is too weak to sufficiently deform the coaxial cable to produce a TDR reflection signal. Growth of this zone is shown in Figure 13 in terms of shear stress values, discussed in the following paragraph.

For further clarity, shear (deviatoric) stress levels in the soil and grout are compared for the two suboptimal behaviors (regions 1 and 3 in Figure 12). As shown in Figure 13, the shear stress in the cable-grout-soil composite approaches failure levels at different locations, corresponding to the relative composite material strengths. Shear stress levels are defined by shading on the side bar and correspond to the amount of shear stress in the material, normalized to the shear strength of the material. Dark zones have reached failure stress. Figure 13a shows the increasing width of the shear stress failure zone in the soil (corresponding to region 3 in Figure 12) as model displacement increases from 0 to 12 mm, for a solid cable in stiff grout, in soft soil. In contrast, shear failure in the weak grout surrounding the solid cable (region 1, Figure 12) is illustrated by the growing size of the dark shading in the grout in Figure 13b as the model displacement increases.

### **Cable and Grout Design**

Two conclusions regarding cable and grout design for TDR applications in soils can be drawn from Figure 12. First, with an optimal cable-grout composite, the braided cable requires less relative displacement of the shear zone to reach the critical shear stress required for TDR response. Secondly, there is an optimal grout to soil strength (stiffness) relationship for generating shear stress in the cables. The relative displacement across the shear band was fifteen millimeters for the calculated results shown in Figure 12, which is important in the evaluation of cable performance. At 15 mm relative deformation, the more flexible, braided cable exceeds the critical shear stress level in the medium and stiff soil types, whereas the solid aluminum cable does not. Although neither cable configuration reaches the critical stress level for soft soils, the braided cable is closer to achieving the critical shear stress level, signaling a higher likelihood of detection in soft soils. Parametric studies show that additional soil shear displacement will cause the shear stress levels to exceed the critical shear stress in both cables.

As shown in Figure 12, the shear stress level in the cables maximizes at optimum grout strength for each soil type. The optimum grout strength is 1 to 5 times the soil strength. Realities of producing grouts in the field restrict this design suggestion to grouts with shear strengths above 250 kPa (unconfined compression strength,  $q_u = 500$  kPa), which is the weakest grout used in the field. It is beneficial to design the grout strength as close to this as possible.

### ***Conclusion***

Differences in observed Time Domain Reflectometry (TDR) reflections in the shear plane in the soft clay beneath a failing landfill lead to three dimensional finite element analysis to determine the optimum cable-grout hole-soil mass properties to maximize these reflections.

A three dimensional finite element model, with an idealized elastic-plastic interaction between the soil-mass, grout, and a TDR cable intersecting a deforming shear zone has provided insight into the behavior and interaction of the components. The complex, three dimensional model involved three different material types (cable, grout, and soil), and two interfaces (cable-grout and grout-soil). The cable and cable-grout interface properties were back-calculated by matching FE calculations to direct shear responses of cable-grout composites. Two realistic cables (braided and solid aluminum outer conductors), one hole size (similar in diameter for a slope inclinometer), and three soil types were investigated. The model was deformed by a prescribed displacement across the slip surface or shear band that was oriented perpendicularly to the cable. Grout strengths were varied in order to find that which sufficiently deformed the cable to produce a critical shear stress (calculated to coincide with the onset of TDR reflection). This process and the associated sensitivity studies required some 100 finite element model runs of the cable-grout composite-soil interaction.

This extended finite element analysis of TDR cable-grout-soil mass composites showed the following trends:

- 1) There is an optimum grout strength and stiffness to maximize the shear stress in a given cable for a given soil strength.



- 2) More flexible, braided cables will generate a TDR response in softer soils with less displacement than the more rigid, solid outer conductor aluminum cable.
- 3) TDR response declines as a result of two material conditions: (a) the grout is sufficiently stronger (stiffer) than the surrounding soil, which prevents the soil from adequately shearing the composite, or (b) weak (compliant) grout lacks the strength and stiffness to cause adequate deformation of the cable for TDR response.
- 4) A ratio of model grout strength to model soil strength of five or less will provide optimal conditions for shearing both cables and avoid smearing the slip surface in soft to medium soils.

### ***Acknowledgements***

The authors are indebted to many individuals and organizations who made this work possible. Financial support was provided by the U.S. Department of Transportation funded Infrastructure Technology Institute of Northwestern University and the Civil Mechanical Systems Division of the National Science Foundation (Grant CMS 23236). Previous work of Richard Cole, Charles Pierce and the other TDR graduate students in the geotechnical program provided the foundation for this study. Field data were provided by GAI Consultants of Monroeville, Pennsylvania and STS Engineering of Vernon Hills, Illinois.

### ***References***

- Bilane, C. (1994). "Effects of Multiple Crimps and Cable Length on Reflection Signatures from Long Cables." M.S. Thesis, Dept. of Civ. and Env. Engrg, Northwestern University, Evanston, IL, USA.
- Blackburn, J.T. (2002). "Finite Element Analysis of TDR Cable-Grout-Soil Mass Interaction During Localized Shearing." M.S. Thesis, Dept. of Civ. and Env. Engrg, Northwestern University, Evanston, IL, USA.
- Plaxis 3D Tunnel User's Manual-Version 1*, Brinkgreve, R.B.J. and Vermeer, P.A. (2001) A.A.Balkema Publishers, Lisse, Netherlands.

- Cole, R.G. (1999). "Compliant TDR Cable/Grout Composites to Measure Localized Soil Deformation." M.S. Thesis, Dept. of Civ. and Env. Engrg, Northwestern University, Evanston, IL, USA.
- CommScope Inc (1998). "Cable Products Catalog." Hickory, North Carolina.
- Dowding, C.H. (1994). "Time Domain Reflectometry for Landslide Surveillance." *Proc., Landslides: Causes, Impacts, and Countermeasures*, H.H. Einstein et.al. Eds., United Engineering Foundation, New York, NY, USA.
- Dowding, C.H., Cole, R.G., Pierce, C.E. (2001) "Detection of Shearing in Soft Soils with Compliantly Grouted TDR Cables." *Proc. TDR 2001*, C.H. Dowding Ed., Infrastructure Technology Institute, Northwestern University, Evanston, IL USA, ISBN 0-9712631-0-8.
- Dowding, C.H. and Huang, F.C. (1994). "Early Detection of Rock Movement with Time Domain Reflectometry." *J. Geotech. and Geoenv. Engrg.*, ASCE, 120(8), 1413-1427.
- Dowding, C.H. and O'Connor, K.M (2000). "Comparison of TDR and Inclinerometers for Slope Monitoring.", *Geotechnical Measurements: Lab and Field; Proc. GeoDenver 2000*, W.A. Marr Ed., ASCE Special Technical Publication No. 106, Reston, VA.
- Ladd, C.C., Foott, R., Ishihara, K., Schlosser, F., and Poulos, H.G. (1977), "Stress-Deformation and Strength Characteristics." *Proc. 9<sup>th</sup> International Conference on Soil Mechanics and Foundation Engineering, Vol. 2, Tokyo*, pp. 421-494
- GAI Consultants, 570 Beatty Rd., Monroeville, PA 15146; Field Data and *Personal Communication with Bruce Roth*.

Model Calibration Results - Physical Parameters				
		Symbol	Solid Aluminum Outer Conductor	Braided Outer Conductor
Cable Shearing Results	Cable Strength <sup>1</sup> [kPa]	$c_{cable}$	4,700 kPa	1,400 kPa
	Cable Modulus of Elasticity <sup>1</sup> [kPa]	$E_{cable}$	300,000 kPa	75,000 kPa
Grout and Interface Parameters	Grout Strength <sup>1</sup> [kPa]	$c_{grout}$	350 kPa	225 kPa
	Grout Modulus of Elasticity <sup>1</sup> [kPa]	$E_{grout}$	75,000 kPa	75,000 kPa
	Interface Strength <sup>1</sup> [kPa]	$c_{interface}$	90 kPa	28 kPa
	Interface Shear Modulus <sup>1</sup> [kPa]	$G_{interface}$	50 kPa	13 kPa
Critical Cable Response	Critical Cable Shear Stress [kPa]	$\sigma_{zy}$ <sup>2</sup>	2000 kPa	350 kPa
	Critical Cable Slope	$\gamma_{zy}$ <sup>2</sup>	0.13	0.065
<sup>1</sup> $c = (1/2) \cdot q_u, \nu=0.2, \phi=0^\circ$				
<sup>2</sup> Using Axes shown in Figure 7, and standard mechanics notation.				

Table 1. Parameters obtained by FE analysis of laboratory tests, employed during FE Analysis of Cable-Grout-Soil interaction.

<b>Grout-Coaxial Cable Composite Shear Test Results</b>				
	<b>Grout Strength, <math>c_u</math>, [kPa]</b>		<b>Grout/Cable Separation [mm]</b>	
	<b>Measured (Unconfined Compression Test)</b>	<b>Acquired by Model Calibration</b>	<b>Measured in Shearing Test</b>	<b>Calculated by FE Analysis</b>
<b>Solid Aluminum Outer Conductor Cable</b>	300	350	12.3	5.8
<b>Braided Outer Conductor Cable</b>	200	225	5.3	2.2

Table 2. Comparison of measured and calculated cable-grout composite shear test results.

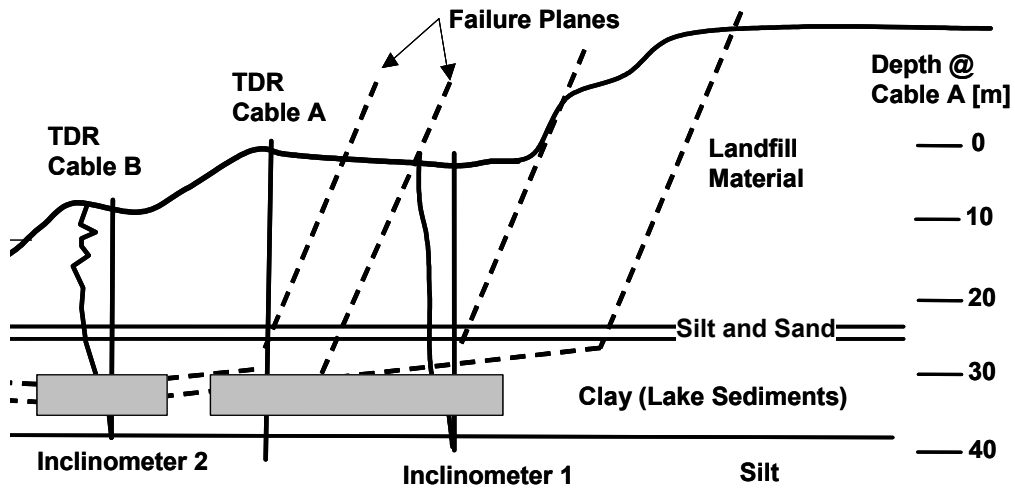


Figure 1. Profile of landfill, showing locations of inclinometers, TDR cables and hypothesized shear failure planes.

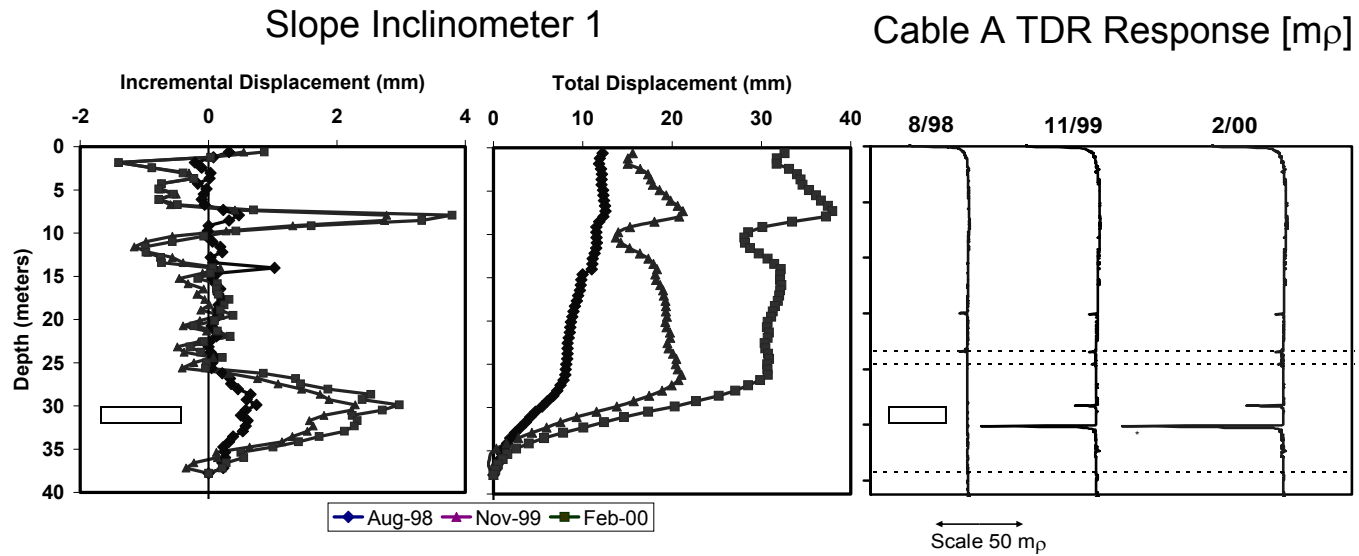


Figure 2. Comparison of slope inclinometer and TDR Cable Response to shear displacement. Shaded rectangle indicates depth of proposed shear zone.

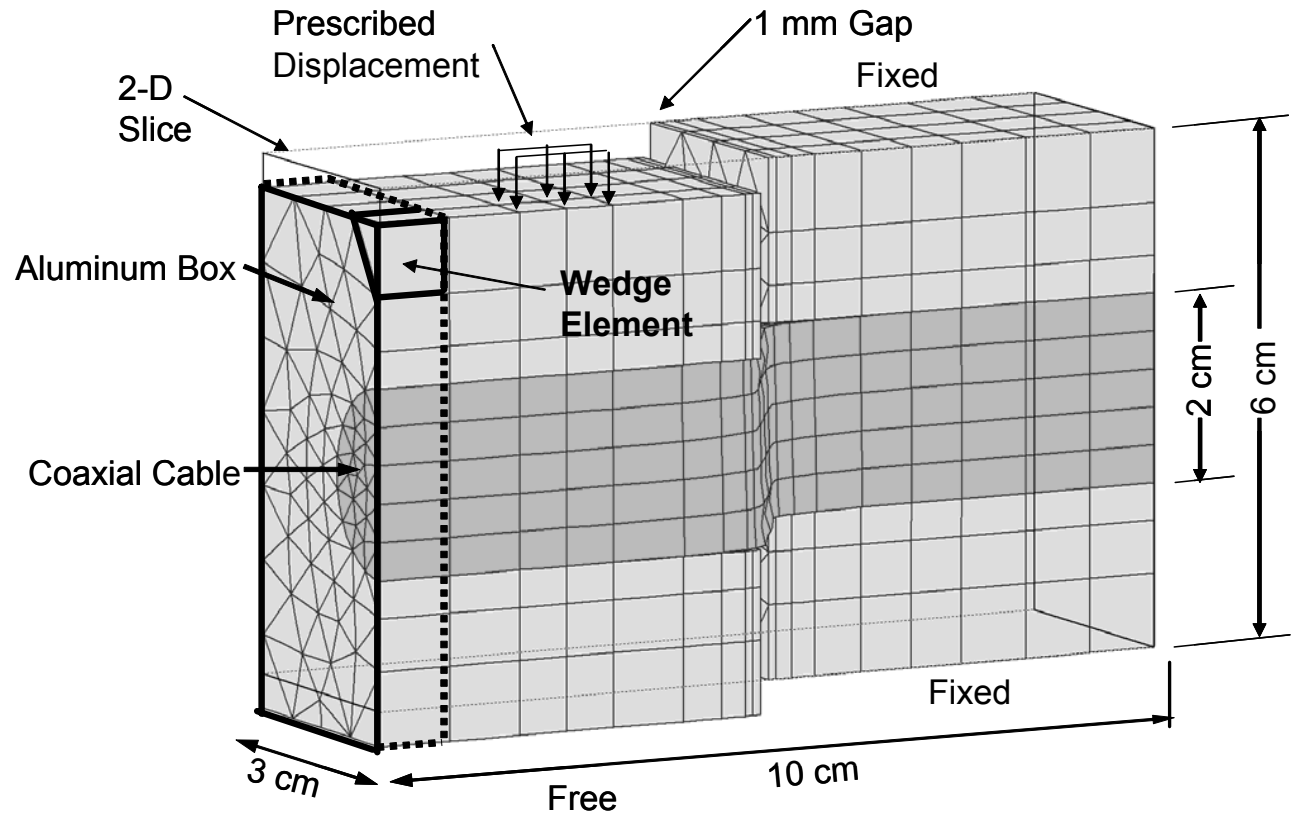


Figure 4. Displaced 3D finite element model of laboratory cable shear test, showing geometry, dimensions, and boundary conditions.

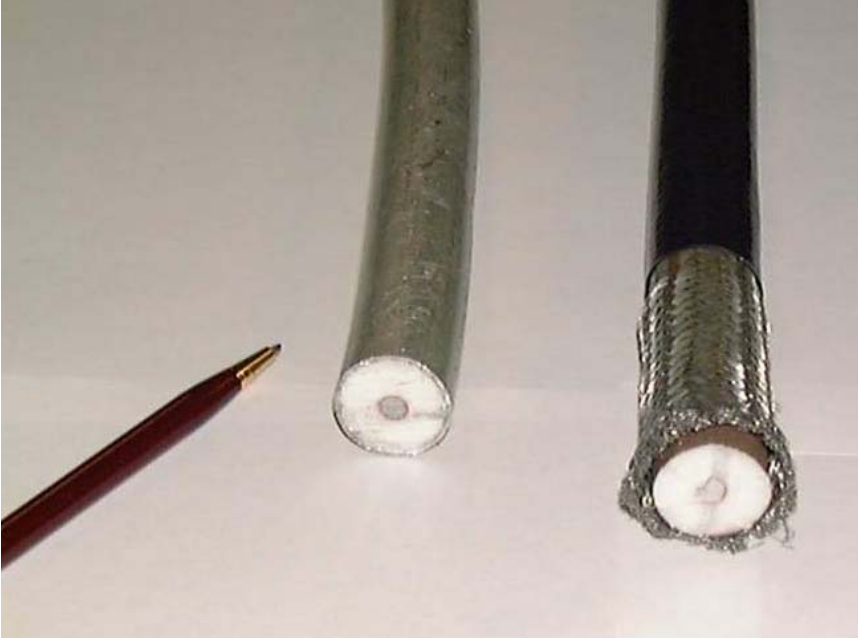


Figure 3. Coaxial cables tested in laboratory: solid aluminum outer conductor on left, braided outer conductor on right.



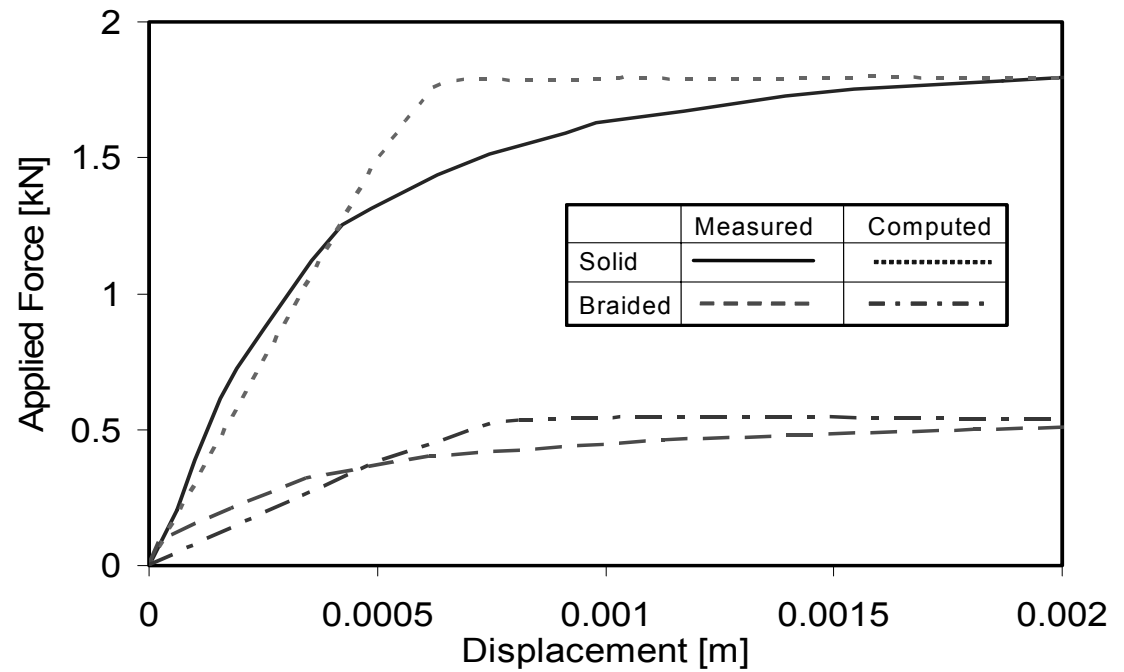


Figure 5. Comparison of measured and calculated force-displacement responses for cable shear test.



Figure 6. Apparatus for shearing cable-grout composites.

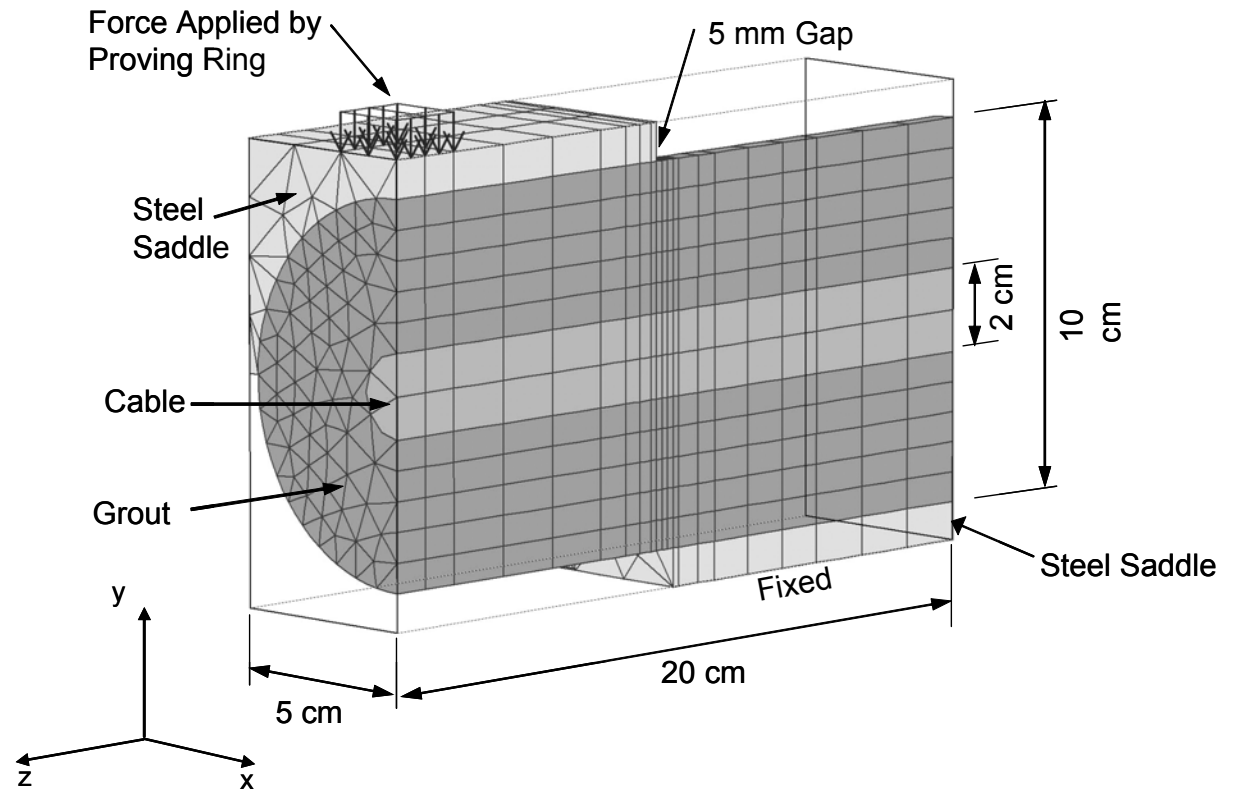


Figure 7. 3D Finite Element Model geometry for cable-grout composite shear test.

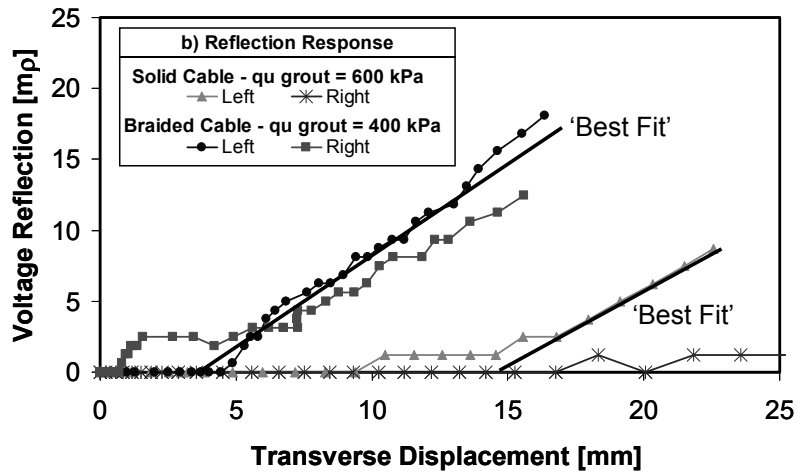
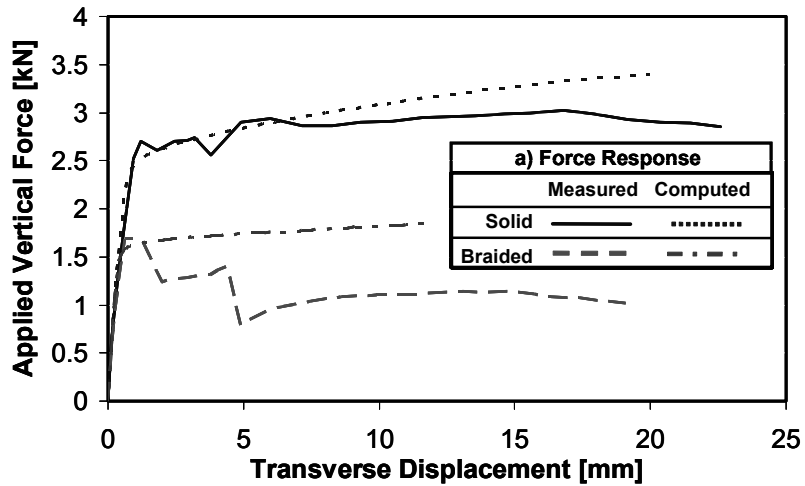


Figure 8. Shear force (a) and Reflection (b) responses of cable from transverse shearing of cable-grout composite.

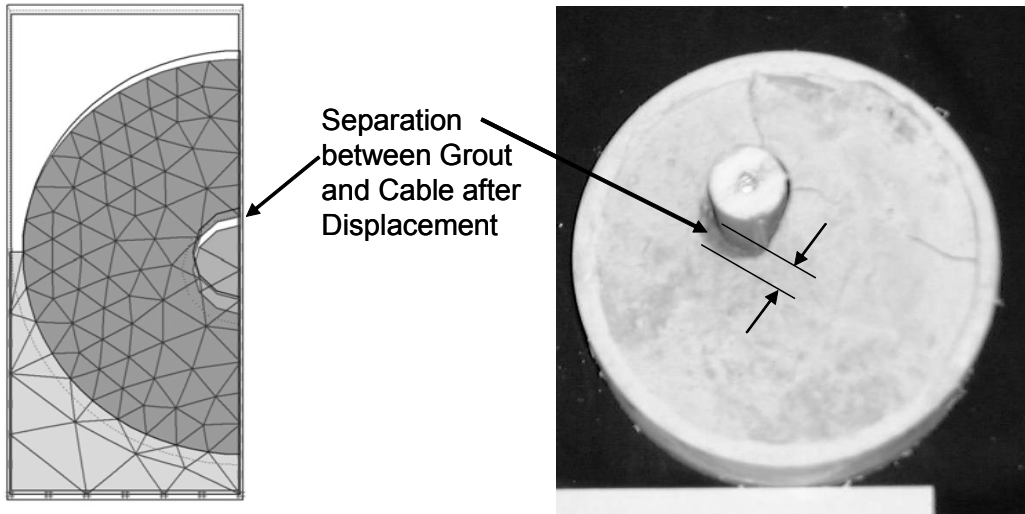


Figure 9. Modeled and observed separation between grout and cable after shear test. The actual cable-grout composite is shown with PVC pipe membrane, which is not modeled.

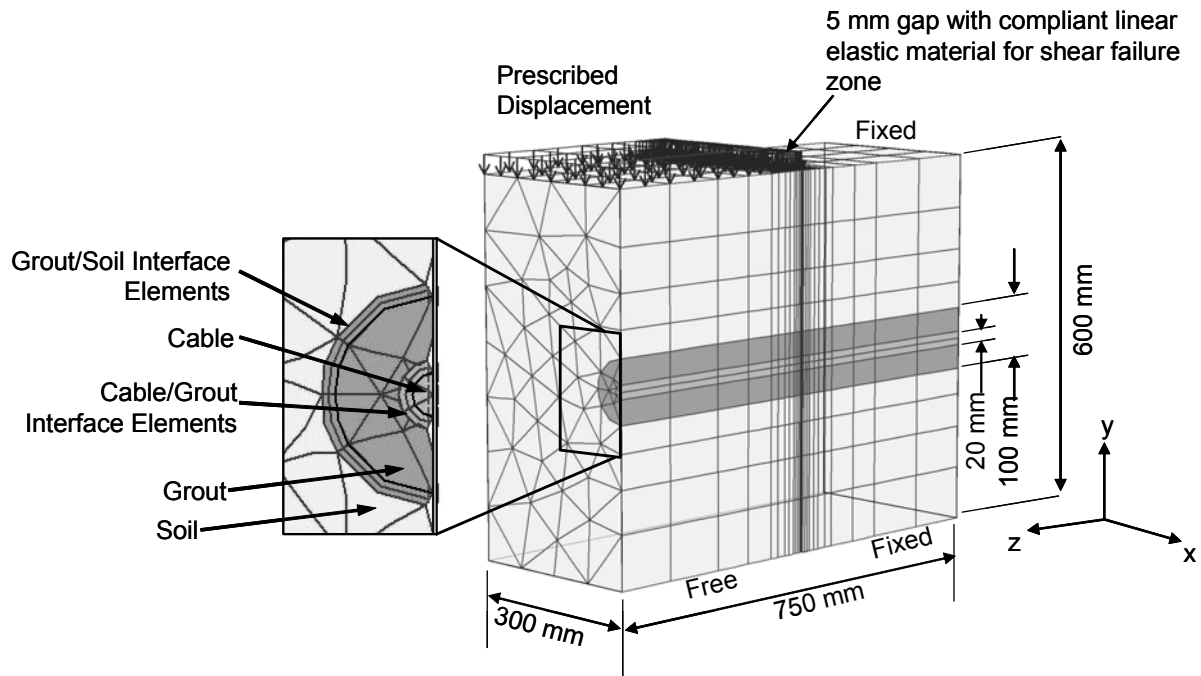


Figure 10. 3D Finite Element Model geometry for cable-grout-soil mass composite.

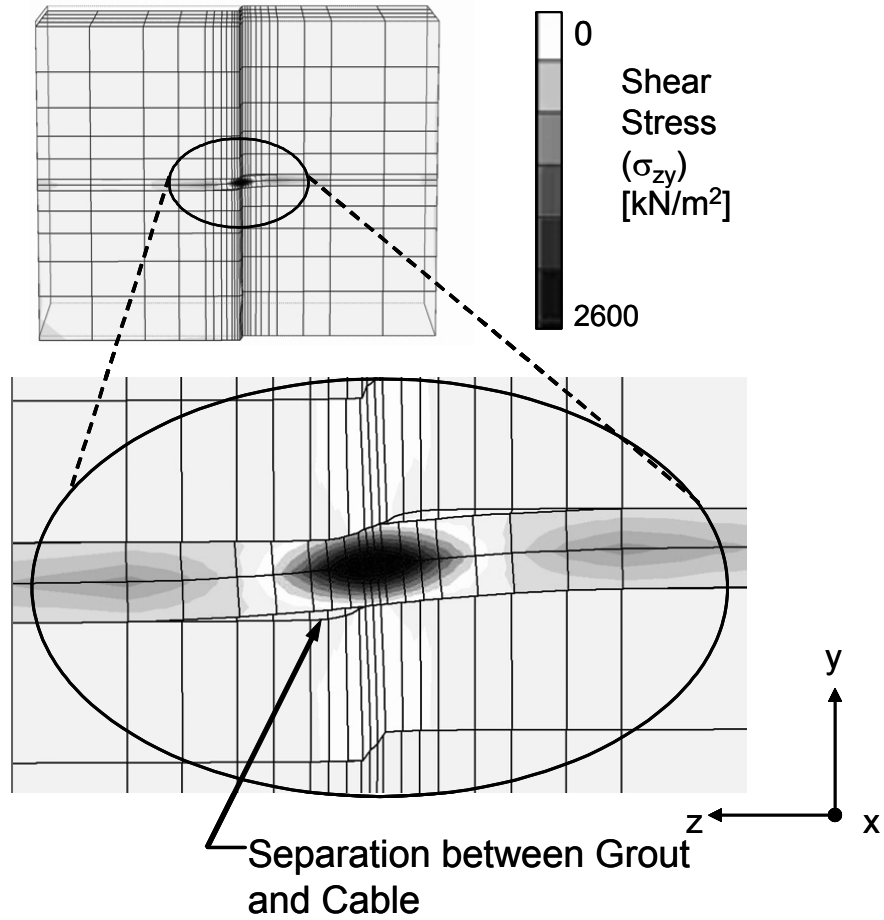


Figure 11. Shear Stress ( $\sigma_{zy}$ ) concentration in cable and cable-grout separation during displacement.

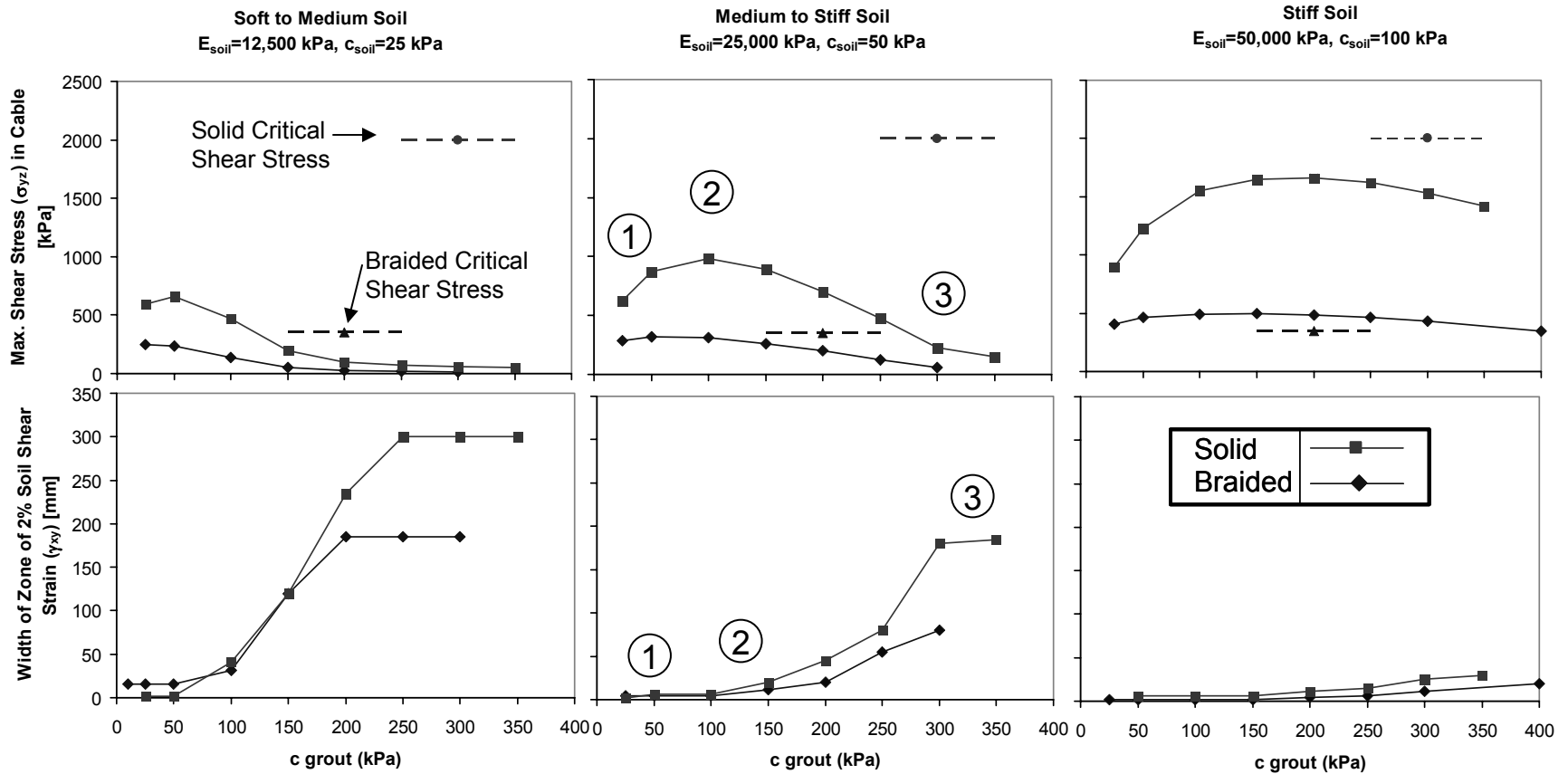


Figure 12. Shear stress level in cable versus grout strength (upper) and width of zone of 2% shear strain versus grout strength (lower). Region 1 involves failure of grout around cable and region 3 involves failure of soil around cable-grout composite, with region 2 the optimum.



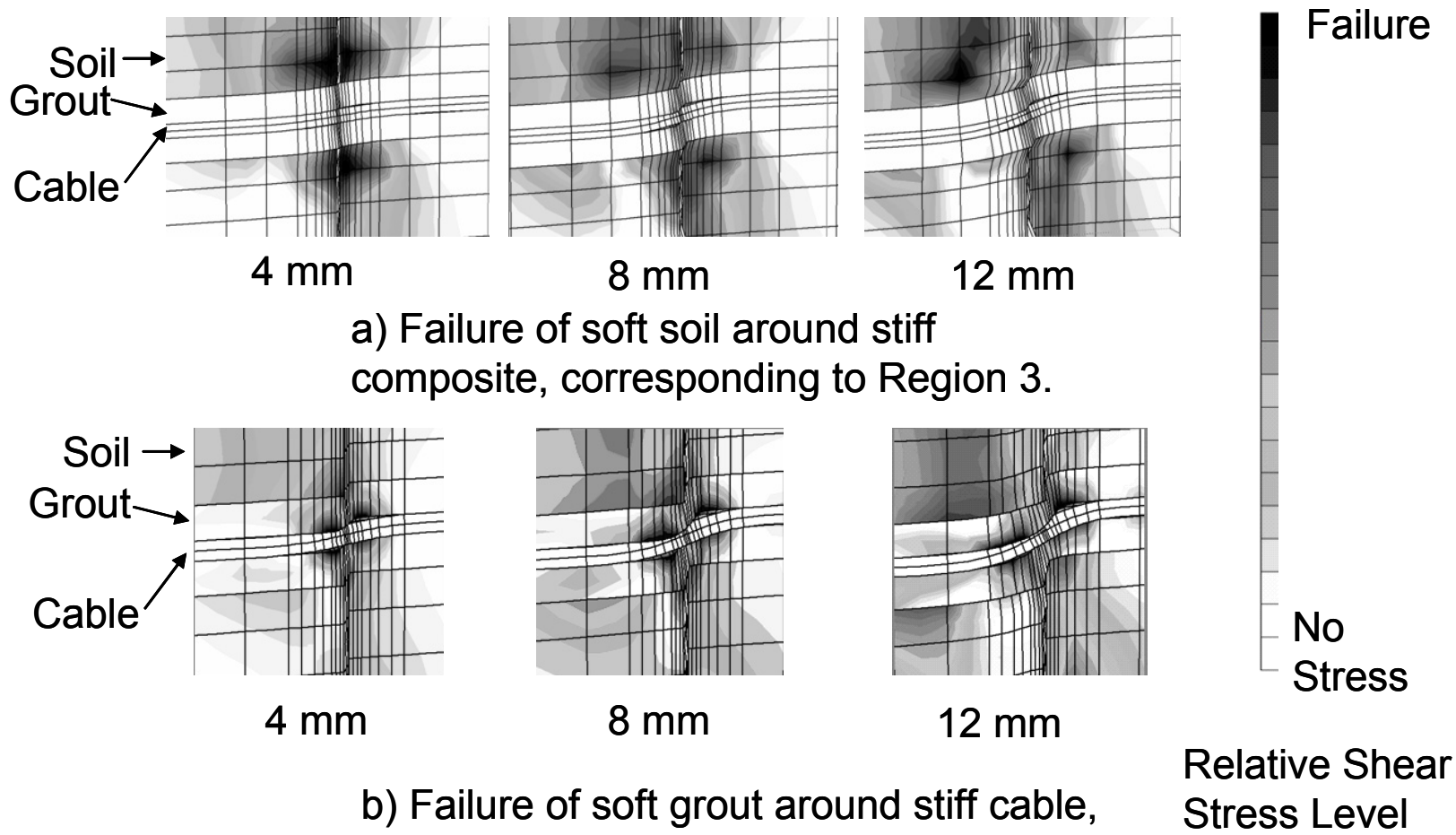


Figure 13. Locations of failure shear stress levels during displacement for: a) relatively soft soil and b) relatively soft grout.